Oxygen incorporation in aluminum nitride via extended defects: Part III. Reevaluation of the polytypoid structure in the aluminum nitride—aluminum oxide binary system

Alistair D. Westwood^{a)}

Soc.

Proc.

and

nced Irich

191

dited Proc.

inov, u. N.

nced

Irich

'ilms,

ymp.

Thin

J.Y.

202,

Thin

cture

nann,
ey &
er. in

by of

ymp.

and

hine,

ymp.

*iistr*v

D.R.

990),

ram.

eport

dited

Proc.

-398

later.

Department of Materials Science and Engineering, Lehigh University, Bethlehem, Pennsylvania 18015

Robert A. Youngman

Carborundum Microelectronics Company, 10409 S. 50th Place, Phoenix, Arizona 85044

Martha R. McCartney

Center for Solid State Science, Arizona State University, Tempe, Arizona 85287

Alastair N. Cormack

New York State College of Ceramics, Alfred University, Alfred, New York 14802

Michael R. Notis

Department of Materials Science and Engineering, Lehigh University, Bethlehem, Pennsylvania 18015

(Received 23 January 1995; accepted 22 June 1995)

This paper extends the concepts that were developed to explain the structural rearrangement of the wurtzite AlN lattice due to incorporation of small amounts of oxygen, and to directly use them to assist in understanding the polytypoid structures. Conventional and high-resolution transmission electron microscopy, specific electron diffraction experiments, and atomistic computer simulations have been used to investigate the structural nature of the polytypoids. The experimental observations provide compelling evidence that polytypoid structures are not arrays of stacking faults, but are rather arrays of inversion domain boundaries (IDB's). A new model for the polytypoid structure is proposed with the basic repeat structural unit consisting of a planar IDB-P and a corrugated IDB. This model shares common structural elements with the model proposed by Thompson, even though in his model the polytypoids were described as consisting of stacking faults. Small additions (~1000 ppm) of silicon were observed to have a dramatic effect on the polytypoid structure. First, it appears that the addition of Si causes the creation of a new variant of the planar IDB (termed IDB-P'), different from the IDB-P defect observed in the AlN-Al₂O₃ polytypoids; second, the addition of Si influences the structure of the corrugated IDB, such that it appears to become planar.

I. INTRODUCTION

Jack and Wilson¹ and Oyama and Kamigaito² are recognized as having independently discovered the group of technologically important engineering ceramics known as "SiAlON's". The ever increasing list of "SiAlON" ceramics take their name from the prototype pseudoquaternary system for this group, Si₃N₄-SiO₂-Al₂O₃-AlN. In the AlN-rich corner of this system, the polytypoid "phases", 8H, 15R, 12H, 21R, and 27R, are found to exist, as shown in Fig. 1.⁴⁻¹⁰ (Polytypoids are crystallographically distinct structures that belong to a subset of the more general classification of polytypism,³ with which the reader is probably more familiar. *Polytypism* is the phenomenon of the existence of an element or compound in two or more

layer-like crystal structures that differ in layer stacking sequence. The layers need not be crystallographically identical, but their chemical composition may not vary by more than 0.25 atoms per formula unit of a constituent element. *Polytypoids* are layer structures whose chemistry may differ from one layer to the next by more than the previously described amount.³) There are small inconsistencies between the various published phase diagrams, concerning the number and the extent of the polytypoid phases.

The polytypoid phases present in the AlN-rich corner of the SiAlON system are based upon the wurtzite crystal structure. It has been generally accepted that the structure of the polytypoid phases in this system and its associated subsystems, e.g., AlN-Al₂O₃ or AlN-Al₂O₃-SiO₂, consist of periodically spaced stacking faults centered on the metal basal planes of the wurtzite lattice, shown in Fig. 2, as originally proposed by Jack,⁴ and corroborated by a number

^{a)}Present address: Union Carbide Technical Center, Bound Brook, New Jersey 08805.

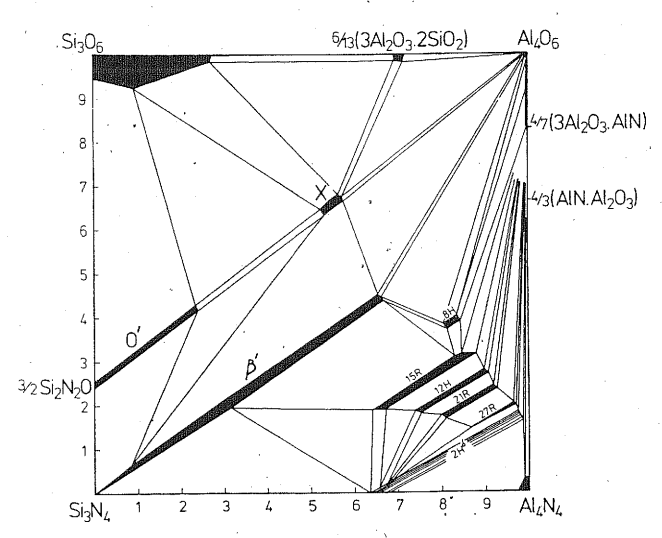


FIG. 1. Phase diagram of the $Si_3N_4-AlN-SiO_2-Al_2O_3$ pseudoquaternary system showing the locations of the polytypoid phases in the AlN-rich corner of the diagram.⁴

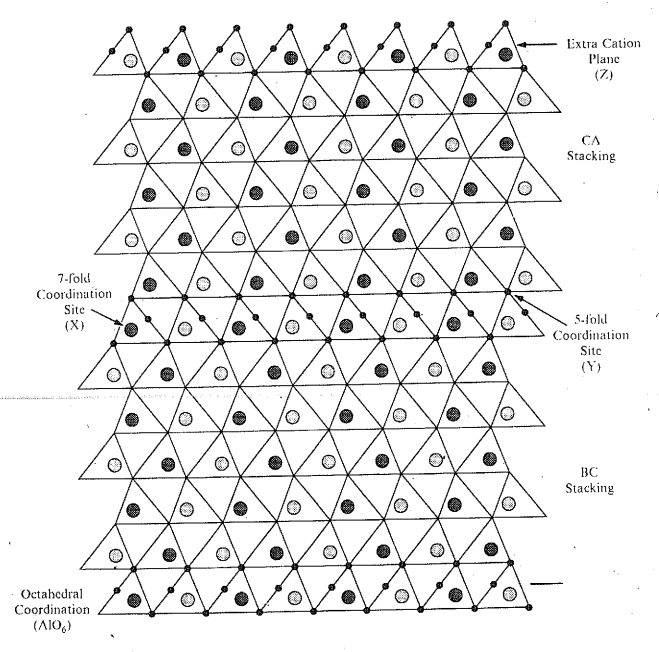


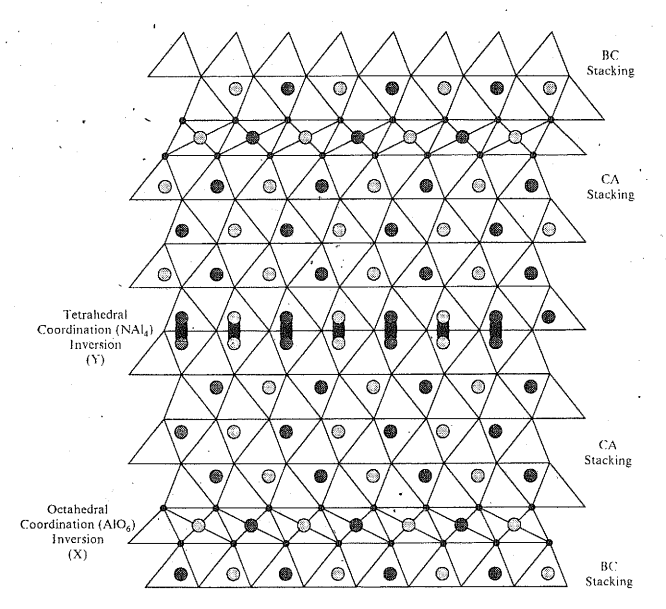
FIG. 2. The polytypoid structure, as first proposed by Jack using x-ray diffraction studies.

of other researchers. $^{7,11-14}$ The wurtzite structure is comprised of two interpretating hexagonal close-packed (hcp) lattices of metal (M) and nonmetal (X) ions, forming cation and anion sublattices. The metal and nonmetal ions are tetrahedrally coordinated with respect to one another in a one-to-one ratio. Within the metal sublattice there are 12 possible nonmetal sites that can be separated into 6 upward- and 6 downward-pointing tetrahedra. To minimize electrostatic repulsion, the nonmetal atoms fill only one type of tetrahedral site. Therefore, polytypoids can exist in two forms: one in which all upward-pointing tetrahedra are filled, and the

other in which all downward-pointing tetrahedra are filled. Jack proposed that the stacking faults form due to changes in the stoichiometry of the metal/nonmetal atom ratio, and that specific nonstoichiometry corresponded to discrete polytypoid phases. The nonstoichiometry occurs because incorporation of Al₂O₃, SiO₂, and Si₃N₄ creates vacancies on the cation sublattice in order to maintain charge neutrality in the crystal. Jack concluded that as the metal/nonmetal atom ratio deviated from the ideal value M/X=1, toward the theoretical limit of M/X = 0.5 (at which point all of the nonmetal tetrahedral sites would be filled), nonmetal atoms would begin to occupy oppositely pointing tetrahedra that share a common base. (The polytypoid phases that are found to exist in the $Be_3N_2-BeO-SiO_2-Si_3N_4$ system exhibit the exact opposite formation sequence. In this system vacancies form on the anion sublattice as the M/Xratio deviates from 1 and moves toward 2, with the stacking faults that form being centered on the nonmetal basal planes. 11,13) This would lead to impossibly short distances between nonmetal atoms. The structure would prevent this unfavorable coordination from occurring by changing the local coordination of the metal sublattice from tetrahedral (hexagonal) to octahedral (cubic), and in so doing, produces a stacking fault. Within this cubic stacked layer, the nonmetal atom tetrahedra no longer need to share a common base, allowing both upwardand downward-pointing tetrahedral sites to be occupied, and thus forming an MX_2 layer. It is generally accepted that the spacing of these MX2 stacking fault layers is determined by the composition of the polytypoid and constrained by charge balance.

Thompson^{12,14} reevaluated the polytypoid structures in the SiAlON system using x-ray diffraction and HRTEM. The revised structure for the family of polytypoid phases is shown in Fig. 3. Surprisingly, the model has been subsequently described as consisting of two planar stacking faults, and therefore considered to be similar to Jack's earlier model.

The accepted structural unit for the polytypoid phases based upon Jack's work (Thompson's revised structure appears to have been ignored), as outlined above, contains unusual structural components. First, 7-fold and 5-fold coordinated metal atom sites exist at, and adjacent to, the stacking faults (labeled X and Y in Fig. 2); both of these coordination numbers are very unlikely for either silicon or aluminum. Secondly, there are basal anion planes adjacent to each other on one side of the stacking fault (labeled Z in Fig. 2); this is an unlikely configuration because of the Coulombic repulsion that would exist between the two anion planes. However, a number of workers¹⁵⁻¹⁸ have investigated the structure of the interfaces in some of the SiAlON polytypoid phases, and in the polytypoid phases found in the AlN-Al₂O₃ pseudobinary, and these data support



are

to

m

led

try

 N_4

to

led

om

nit

etal

uld

are

ind

ihit

em

/X

the

etal

OT

uld

by

ice

and

bic

ger

ırd-

.ed.

ted

is is

and

ires

and

of

the

ζof

1 to

юid

sed

ned

irst.

xist

and

are

dly,

on

this

ihic

nes.

ated

ON

und

port

FIG. 3. The refined model of the polytypoid structure proposed by Thompson. The two different types of interface are marked, and an inversion across both interfaces is clearly apparent. The black ovals represent those tetrahedral sites that share an aluminum ion.

the structure proposed by Jack.⁴ Even with these highly unlikely structural components, recent work¹⁹ still quotes Jack's paper as the authoritative study on polytypoid structures, and they ignore all subsequent work by Thompson and coworkers.^{7,11,12,14}

Recently, investigations by a number of researchers²⁰⁻³¹ have led to a detailed understanding of the mechanism by which oxygen is incorporated in the AlN lattice. In the original work by Slack, 32 a reaction describing the incorporation of oxygen into the AlN lattice was proposed in which an aluminum vacancy $(V_{A1}^{"'})$ would be created for every three oxygen atoms sitting on nitrogen sites (ON) in order to maintain charge neutrality. Harris et al.23 further developed this model to show that an aluminum vacancy and an oxygen ion formed a defect complex $(O_N^{\bullet} - V_{A1}^{"})$ bound by Coulombic attraction; furthermore, above a critical concentration of ~0.75 at. % oxygen, the mechanism of oxygen incorporation switched from randomly distributed defect complexes $(O_N^{\bullet} - V_{Al}^{""})$ to octahedrally coordinated complexes consisting of an aluminum surrounded by six oxygens sitting on nitrogen sites (O_N-Al)_{oct}. These octahedral complexes can then form extended two-dimensional defects, via coalescence of these complexes and precipitation onto the basal plane (see Fig. 9 in Ref. 23). Precipitation of the octahedral complexes produces an aperiodic distribution of planar and curved inversion domain boundaries (IDB's). 25-30 The microstructure continues to evolve as the amount of oxygen incorporated in the AlN lattice increases. With continued oxygen incorporation, the aperiodic distribution of planar and curved IDB's is

replaced by a quasiperiodic array of planar and curved IDB's, and this ultimately evolves into the polytypoid structures. Increasing oxygen addition finally results in the formation of γ -AlON spinel. Figures 4(a)-4(d) show the effect of increasing oxygen incorporation into the AlN lattice.

It appears that the above description concerning the evolution of the extended defects in AlN due to oxygen incorporation contradicts the generally accepted structure (i.e., Jack's) of polytypoids. This body of recent work suggests that the structure of the polytypoid phases are comprised of arrays of IDB's, rather than the previously accepted arrays of stacking faults. There are two interesting possible explanations. First, if the polytypoid phases are arrays of stacking faults, some mechanism is required that would allow an IDB (which is crystallographically defined as an inversion interface) to transform to a polytypoid structure composed of stacking faults (which are defined as translation type interfaces). 25,33 This transformation would require the removal of the inverted portion of the crystal, and subsequent large structural rearrangement. The presence of such a transformation is inconsistent with all the experimental evidence that shows a progressive sequence of events, from oxygen point defect and aluminum vacancy creation, to the formation of planar and curved IDB's, to periodic defect structures. Therefore, the sudden transformation of IDB's into arrays of stacking faults does not follow this progressive sequence. The alternative explanation proposed here is that the polytypoid phases are in fact comprised of IDB's, contrary to the accepted stacking fault model.

Close inspection of Thompson's 12,14 revised model of the polytypoid structure, as shown in Fig. 3, reveals considerable differences between this model and Jack's earlier model. First, the obvious difference is that there are two structurally different interfaces in the revised model rather than the single, simple, oxygen-rich stacking fault as in Jack's model. Second, an inversion in the wurtzite structure occurs across the octahedrally coordinated units comprising the first interface (labeled X in Fig. 3). Also, a crystallographic inversion operation exists at the second interface (labeled Y in Fig. 3) that inverts the wurtzite structure back to its original orientation. The second interface has only half the available metal atom sites filled, and therefore contains a high metal vacancy concentration. The first interface exhibits a translation of $\mathbf{R} = 1/3\langle 10\overline{1}0 \rangle + x\langle 0001 \rangle$, and the second interface has a translation of only $\mathbf{R} = x(0001)$. These two interfaces proposed in Thompson's model show remarkable similarity to the structures observed for the planar and curved IDB's described in Parts I and II of this paper. 29,30 It should be noted that interfaces characterized by an inversion operation, i.e., inversion domain boundaries, are crystallographically distinct from those

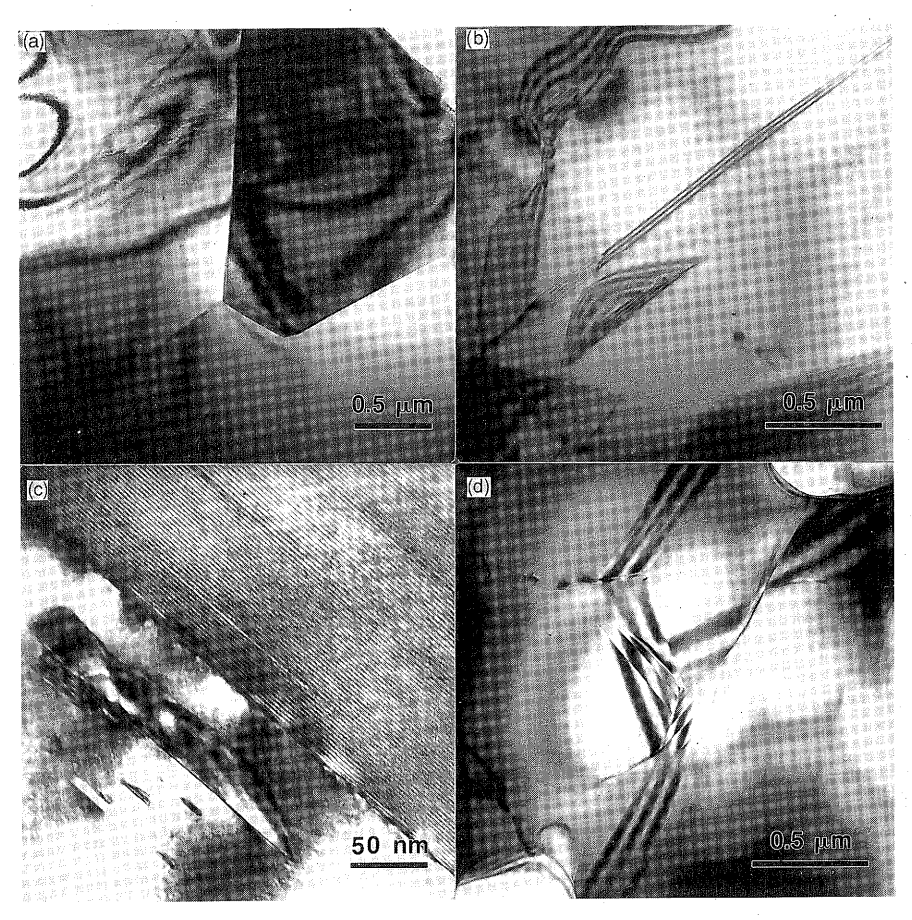


FIG. 4. Increasing oxygen concentration on moving from (a) to (d) shows (a) a clean defect-free AlN microstructure, (b) the formation of random isolated IDB's (c) polytypoids, and finally (d) the cubic γ -AlON structure.

characterized by translational symmetry, i.e., stacking faults, and they are not identical. The use of symmetry for classifying interfaces is used because it removes any ambiguity associated with other forms of interface definition. An inversion boundary can additionally have translational symmetry superimposed upon the inversion symmetry. The characteristics of a material containing inversion interfaces may be very different to a material containing purely translational interfaces, and thus the need for differentiating between the two interface types is necessary.

These analyses conclude that the revised model proposed by Thompson^{12,14} should be correctly described as being comprised of two dissimilar inversion domain boundaries. The two models proposed by Jack and Thompson are in fact structurally very different. Misclassification of Thompson's model as consisting of stacking faults has caused the structural differences between the two models to have been largely overlooked. As a result, the accepted structure of polytypoids being composed of stacking faults has not been challenged or fully investigated.

Part III of this paper will therefore focus on careful identification of the structures of the polytypoids present

in the AlN-Al₂O₃ pseudobinary materials, and also on the structure of the polytypoid phases in the AlN-rich corner of the SiAlON pseudoquaternary phase diagram. This work will show that the long-held belief that the polytypoid structures are arrays of periodic stacking faults is incorrect.

II. EXPERIMENTAL PROCEDURE

A. Sample preparation

To investigate the structure of the polytypoid phases in the $AlN-Al_2O_3$ pseudobinary phase diagram, three $AlN-Al_2O_3$ compositions were prepared, 90 wt. % AlN-10 wt. % Al_2O_3 , 85 wt. % AlN-15 wt. % Al_2O_3 , and 80 wt. % AlN-20 wt. % Al_2O_3 , using high-purity Al_2O_3 powder (Biakowski CR-30) and AlN powder (Tokuyama Grade F) containing ≈ 1.0 wt. % oxygen, and cation impurities totaling <400 ppm. The polytypoid phases in the AlN-rich corner of the SiAlON diagram were investigated by preparing samples that contained AlN, Al_2O_3 , and SiO_2 . Three compositions were chosen: 90 wt. % AlN-9.0 wt. % $Al_2O_3-1.0$ wt. % SiO_2 , 90 wt. % AlN-9.5 wt. % $Al_2O_3-0.5$ wt. % SiO_2 , and 90 wt. % AlN-9.8 wt. % $Al_2O_3-0.2$ wt. % SiO_2 .

Powder processing was conducted in a dry box, in which the moisture content was maintained below 10 ppm $\rm H_2O$, minimizing further oxygen pickup during processing. The samples of the various compositions were cold pressed, forming 1.0 cm diameter pellets. Each sample was then placed in an AlN crucible and loose AlN powder was packed around the pellet. The samples were pressureless sintered at 1975 °C, for 4 h, in a $\rm N_2$ atmosphere, and then furnace cooled.

Samples were prepared for electron microscopy by cutting thin slices from the fabricated bulk samples using a diamond saw, followed by ultrasonically cutting 3.0 mm disks out of the slices. These disks were then dimpled to a final thickness of $\approx 10-20~\mu m$. The sample was ion beam thinned to perforation using 4 kV Ar ions at a grazing incident angle of $10^{\circ}-12^{\circ}$.

B. Instrumentation

1 of

on

ich

ım.

the

ing

ses

ree

. %

 O_3 ,

rity

der

and

oid

am

ned

ere

. %

 O_2 ,

 O_2 .

Conventional transmission electron microscopy (CTEM) was conducted on a Philips 400T microscope equipped with a LaB₆ electron source and operated at 120 kV. Conventional and high-resolution transmission electron microscopy (HRTEM) was conducted on a JEOL JEM-4000EX microscope fitted with a LaB₆ filament and operated at 400 kV. The use of the high resolution top-entry double-tilt specimen stage allowed $\pm 20^{\circ}$ of tilt. The optical parameters of the microscope used in image simulation calculations were spherical aberration constant $(C_s) = 1.00$ mm, beam convergence semi-angle $(\alpha) = 0.5$ mrad, and an electron beam focal spread $(\Delta f) = 8.0$ nm. The interpretable resolution of this microscope at Scherzer defocus (-49.7 nm) was 0.17 nm point to point.

The authors refer the reader to paper I for a detailed description of the atomistic computer simulations.²⁹

III. OBSERVATIONS AND RESULTS

A. Conventional transmission electron microscopy (CTEM)

The microstructures observed in the three AlN-Al₂O₃ compositions consisted of a large number of AlN grains that contained isolated curved and planar IDB's, and a smaller number of polytypoid grains. There were also grains such as that shown in Fig. 5 that show a mixed defect population, with individual planar and curved IDB's (left-hand side) and which gradually evolve into large spacing "disordered" polytypoid structures (right-hand side). Disordered polytypoids are defined as those regions that possess an irregular spacing between defects. Grains with a mixed defect population provided great insight into the transformation from planar and curved IDB's into a microstructure composed of periodic faults that resemble the polytypoid phases.

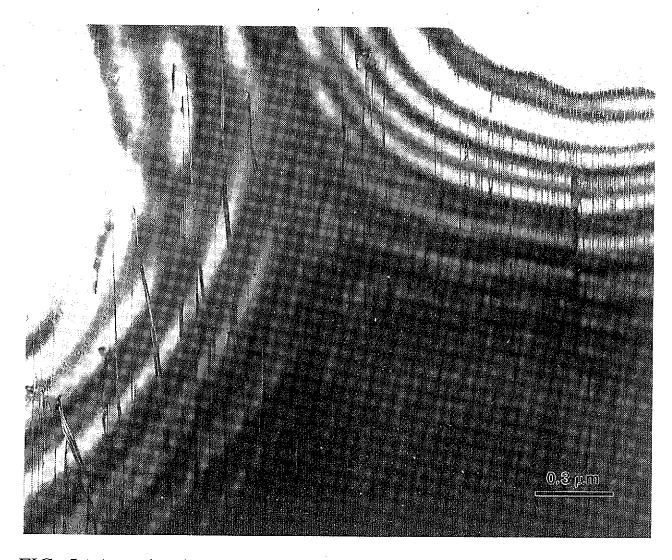


FIG. 5. A grain showing the gradual transition from isolated curved and planar IDB's on the left, to regular arrays of planar and corrugated IDB's on the right. On moving left to right, the curved IDB becomes more constrained and consequently more planar.

The planar and curved defects that are present on the left-hand side of Fig. 5 show the characteristic morphology of isolated IDB's in AlN.^{20–25} On moving toward the right-hand side of Fig. 5, the spacing between the planar IDB's decreases. This has a dramatic effect on the morphology of the curved IDB; as the distance between planar IDB's decreases, the curved IDB's gradually become more planar. Using conventional two-beam imaging methods, the displacement vector **R** for the curved IDB was investigated and was found to have only a *c*-axis displacement, with no basal plane translation. This is the same result as previously reported,²⁴ indicating that the structure of the curved IDB interface does not dramatically change even when its morphology is quite different.

Utilizing the failure of Freidel's law for polar crystals, Serneels et al.34 and Snykers et al.35 showed that a striking contrast reversal occurs between domains separated by a crystallographic inversion operation, when the crystal is imaged under a multibeam condition, e.g., using a polar reciprocal lattice vector (for AlN, $g_{(0002)}$ or $g_{(10\overline{1}1)}$) along a low index zone axis. Using this technique, it was confirmed that the disordered polytypoid structure shown on the right-hand side of Fig. 5 is comprised of inversion domain boundaries; the striking contrast reversal across the boundaries is clearly evident in Fig. 6. This result indicates that the second interface lying between the planar IDB's, and originating from the curved IDB, still contains an inversion operation. The morphology of this second type of inversion interface is corrugated and with varying width. The overall nonperiodic nature of the disordered polytypoid region is evident; however, embedded within

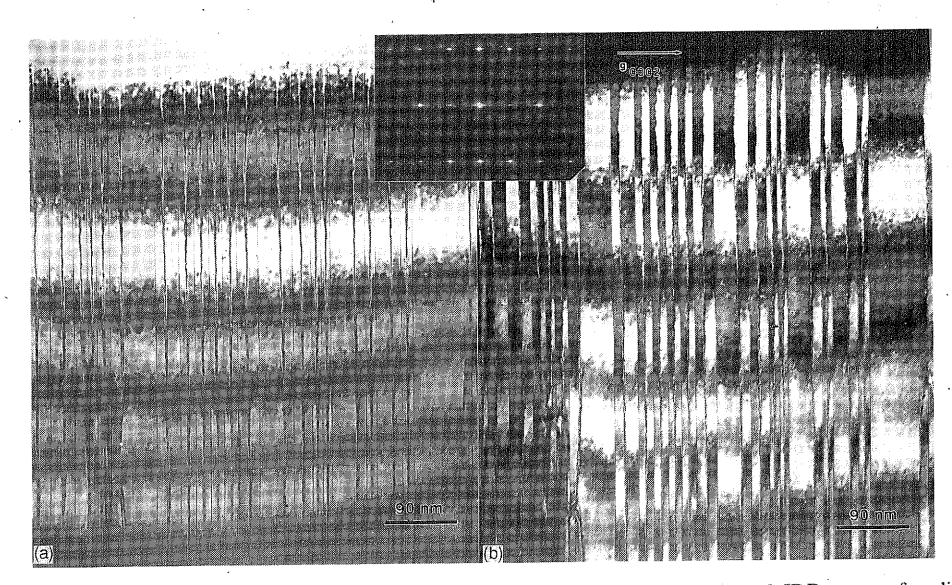


FIG. 6. (a) Bright-field image from the right-hand side of Fig. 5 showing the planar and corrugated IDB array of a disordered polytypoid. (b) Dark-field image using a $g_{(0002)}$ polar reflection under a multibeam condition along the $\langle 1\overline{2}10 \rangle$. The contrast reversal on crossing the corrugated and planar IDB's clearly shows that an inversion operation occurs across these boundaries. A $\langle 1\overline{2}10 \rangle$ diffraction pattern from the area of interest clearly shows streaking in the $\langle 0002 \rangle$ which suggests variable IDB spacing.

these regions are smaller regions of perfectly ordered polytypoid structure, as seen in Fig. 6.

B. High-resolution transmission electron microscopy (HRTEM)

A grain comprised of an ordered polytypoid phase with some very small amount of disorder can be seen in Fig. 7. Figure 8 shows a HRTEM image obtained along a $\langle 11\overline{20} \rangle$ from such a typical polytypoid region. The most obvious feature in this micrograph is the regularly spaced, planar IDB's. They have been analyzed in detail and were found to be identical with the planar IDB structure previously documented, 27,30 which consists

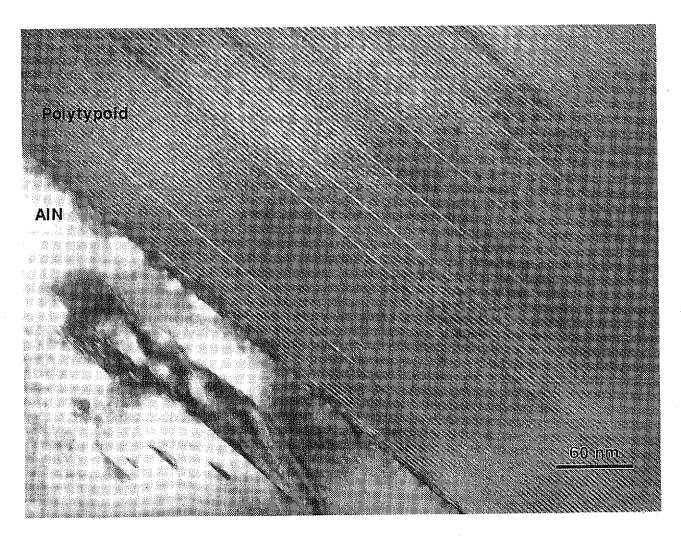


FIG. 7. An ordered polytypoid grain in the $AlN-Al_2O_3$ sample with a strained interface with an AlN grain containing small "D" shaped defects comprised of curved and planar IDB's.²⁵

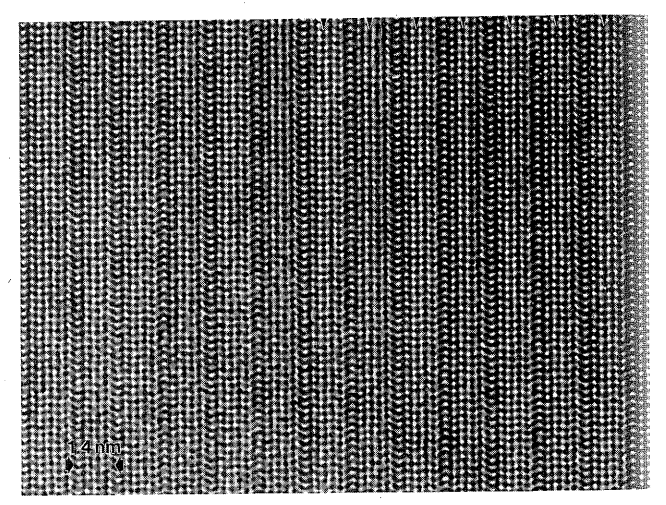


FIG. 8. A HRTEM micrograph of an $AlN-Al_2O_3$ polytypoid clearly showing the planar IDB's, and a second contrast feature consisting of two bright rows (arrowed) between the planar faults.

of a plane of octahedrally coordinated aluminum ions bound to oxygen and nitrogen ions in a ratio of 3:1. On viewing Fig. 8, it appears that the corrugated IDB clearly visible in Fig. 6 has disappeared. However, close inspection of Fig. 8 reveals the presence of a second less distinct feature separating the planar IDB's; this feature is a double row of higher intensity white dots clearly present on the right-hand side of the image. This same feature is clearly visible in Fig. 9, which is an HRTEM image taken under slightly different imaging conditions than those used in Fig. 8, and clearly shows the diffuse corrugated nature of this feature. A pair of dark-field micrographs in Fig. 10 show the same region of polytypoid, imaged using opposite {0002} polar

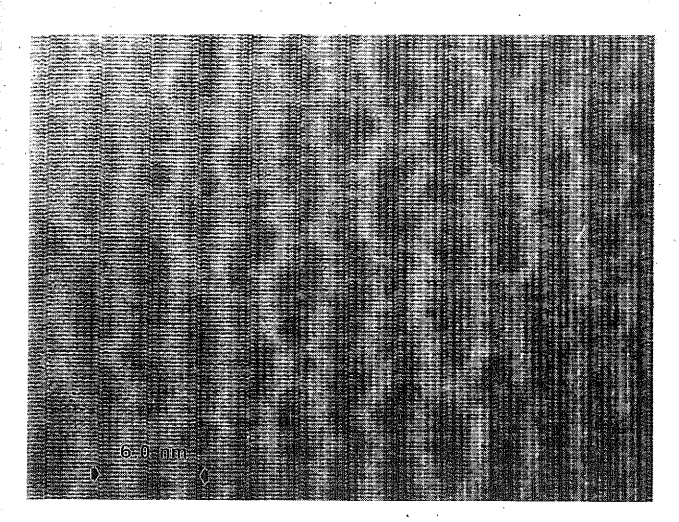


FIG. 9. A HRTEM image obtained using different imaging conditions from those in Fig. 8, clearly showing the diffuse corrugated contrast of the feature lying between the planar IDB's.

oid.

the

the

g of

ons

3:1.

DB

ose

ond

this

lots

This

ging

wS

pair

ıme

olar

an

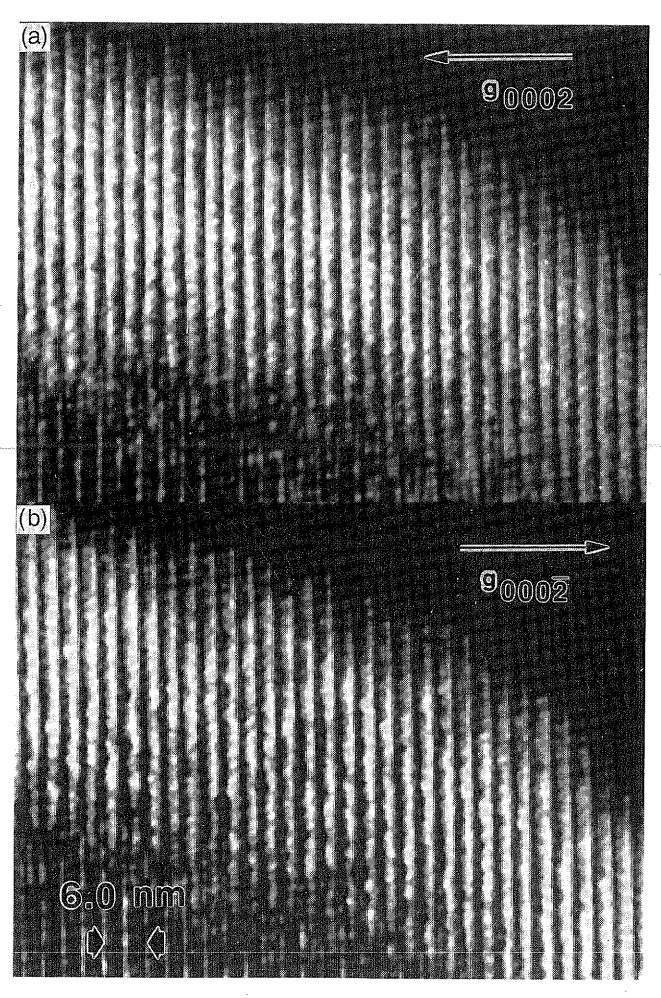


FIG. 10. A DF pair obtained using opposite polar reflections under a multibeam imaging condition along the $\langle 11\overline{2}0\rangle$: (a) $g_{(0002)}$ and (b) $g_{(000\overline{2})}$. The corrugated IDB can be seen clearly lying between the planar IDB's.

reflections. These images confirm that the corrugated structure with diffuse contrast, lying between the planar

IDB's in the polytypoid structure in Fig. 8 and 9, is due to the corrugated IDB. Therefore, the polytypoid structure in the AlN-Al₂O₃ system are comprised of a repeat unit consisting of a planar and a corrugated IDB.

C. Atomistic computer simulations

The initial intent of the investigation was to study the original model of Jack⁴ which has been supported by Van Tendeloo et al., 15 Bando et al., 16 and Krishnan et al.17 Therefore, the model proposed by Jack was used as the initial input supercell structure for the calculations. The 5-fold and 7-fold coordinated metal atom sites, and the two adjacent anion planes next to the stacking fault layer as shown in Fig. 2, were found to be unstable components in this structure. The calculated relaxed structure, based upon minimum strains between the atoms, is presented in Fig. 11(a). A mixed Al-N, O plane forms at the location of the adjacent anion planes, the 7-fold coordinated aluminum site is lost, and the 5-fold site becomes more symmetrical. This result supports the experimental evidence that indicates that the model proposed by Jack is not the preferred structure. A development of this result was to take the lower portion of Fig. 11(a) (labeled A) and invert it to create two structurally different IDB interfaces. The cohesive energy of this structure, shown in Fig. 11(b) was greater than Fig. 11(a), and much larger than the original structure of Jack, implying a much more stable structure. The observation that the simulation provided the relaxed structure of Fig. 11(a), rather than that shown in Fig. 11(b), suggests that Fig. 11(a) represents a metastable structure.

There are two similarities between Thompson's model, shown in Fig. 3, and the calculated interface structures for the IDB's, shown in Fig. 11(b), and in the previous work detailing the simulation of the planar and curved IDB's. 29,30 The octahedrally coordinated interface in Thompson's model is very similar in structure to the planar IDB described in these papers. The second interface in Thompson's model, labeled Y in Fig. 3, is identical to the initial starting structure for the atomic simulations of the curved IDB.³⁰ In those calculations the initial curved IDB structure consisted of nitrogen trigonally coordinated with six aluminums, this changed, with the final structure comprised of an Al-N mixed plane surrounded by oxygen and vacant aluminum sites, resulting in an interface with a distorted aperiodic structure. It is suggested that the regular periodicity of the second interface in Thompson's model would become distorted due to electrostatic repulsion from closely spaced like ions, or from the presence of aluminum vacancies causing distortion of the local lattice. Further calculations are required to elucidate the polytypoid structures in the AlN-Al₂O₃ and SiAlON systems.

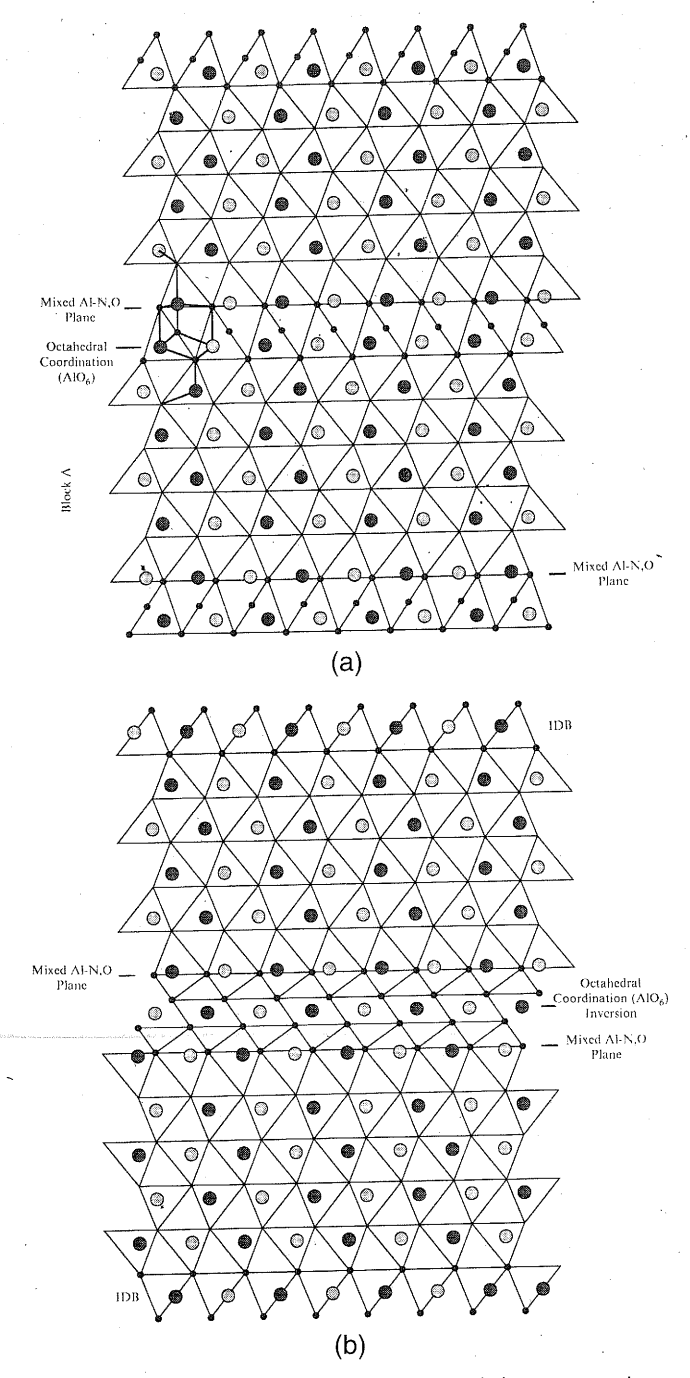


FIG. 11. (a) The structure output from the atomistic computer simulations, the original stacking fault structure, 7- and 5-fold coordinated sites, and adjacent anion planes are removed, being replaced by a mixed anion-cation plane. (b) shows the output structure when the bottom block in (a) is inverted, creating two structurally different IDB's. The input structure was very similar to the output structure. The overall energy of the system was reduced on moving from Jack's model in Fig. 2, through (a) and finally to (b), corresponding to an increase in stability. These structures should be compared with Jack's model in Fig. 2.

D. Silicon additions

The effect of silicon additions on the structure and formation of polytypoids was investigated by

comparing the results from the $AlN-Al_2O_3$ samples to those from the silicon-containing $AlN-Al_2O_3-SiO_2$ samples. The microstructures of the silicon-containing samples were found to be surprisingly different from the $AlN-Al_2O_3$ samples. The silicon-containing samples had a high proportion of ordered polytypoid grains; no grains were observed that contained any isolated curved or planar IDB's.

HRTEM studies revealed a far more complex structure for the silicon-containing polytypoid phases than those observed for the AlN-Al₂O₃ polytypoid phases. A through-focal-series reconstruction of a 20 member series was made from images of a silicon-containing polytypoid; the phase image is shown in Fig. 12. This method³⁶ allows for the retrieval of both the phase and amplitude of the electron image wave. This complex wave then may be corrected for spherical aberration and defocus so that the phase and amplitude of the electron wave at the exit surface of the crystal are revealed. If the sample is "thin enough", the phase image may then be directly interpreted in terms of the projected potential of the atomic columns with white dots representing regions of high potential. The phase image provides a number of interesting observations. First, there are two distinctly different planar IDB's, one exhibiting similar contrast and width to the previously documented planar IDB (labeled IDB-P), and a second planar IDB of different contrast (much more diffuse) and width (labeled IDB-P'). Second, the corrugated IDP is not visible between the two different types of planar IDB. Third, as shown at the top of Fig. 12, the alternating sequence of the two different planar IDB's is sometimes lost, with only the IDB-P appearing to be present.

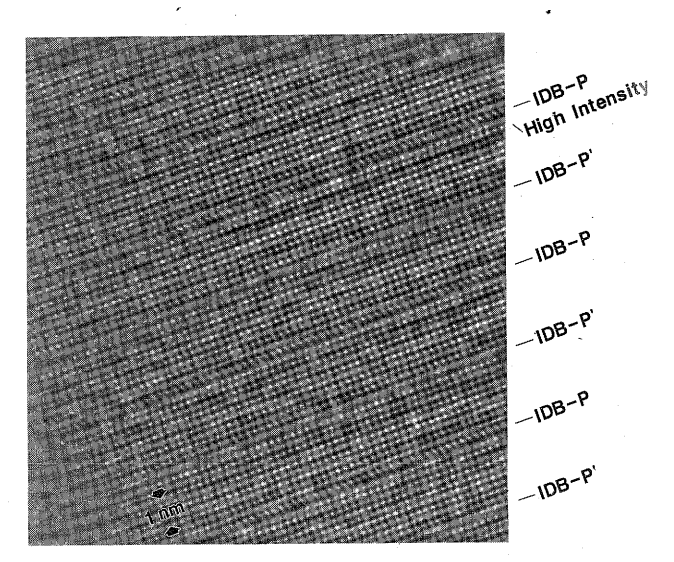
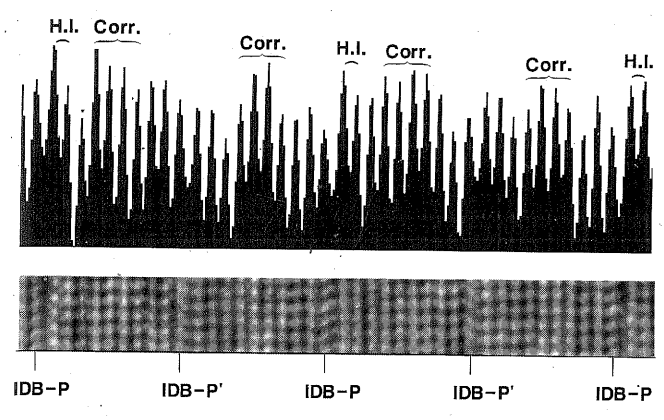


FIG. 12. Phase image from through-focal-series reconstruction of a silicon-containing polytypoid. The previously documented planar IDB is labeled as IDB-P, and the new second type of IDB is labeled as IDB-P'. The two bright basal planes adjacent to IDB-P are indicated as High Intensity.



 O_2

.ng om

ng bid

ıny

ıc-

ian es.

ber

ng

his

ınd

lex

ınd

on

the

be

of

ons

ber

tly

ast

DВ

ent

ıB-

en

wn

wo

the

ity,

DB

1 as

ited

FIG. 13. Top: Histogram of the intensities of the atomic planes. Bottom: The structure from which the histogram originated. The regions of higher intensity are labeled on the histogram, indicating the possible location of the corrugated IDB (Corr.), and the two brighter basal planes adjacent to the IDP-P are labeled as H.I.

Further details of the structure are revealed in Fig. 13, which is a histogram of the intensities of the atomic planes matched up with the image. First, the IDB-P consistently shows two planes adjacent to the IDB that are of greater intensity; these two planes are always on the same side of the IDB. Second, an additional high intensity region is always present across 2-4 planes between adjacent planar IDB's. This could possibly be some indication of the existence of the corrugated IDB. Finally, the IDB-P' is asymmetrically positioned with respect to its adjacent planes and is wider than the IDB-P. The polytypoid structures observed in the AlN-Al₂O₃-SiO₂ system, when compared with those found in the AlN-Al₂O₃ system, clearly indicate that the presence of silicon exerts a strong influence on controlling the final polytypoid structure. A comparison between the effect of silicon and oxygen on polytypoid formation reveals that with ~5 wt. % oxygen the microstructure contains very few polytypoid grains, some mixed grains containing disordered arrays of IDB's, and a large number of grains with isolated IDB's. The addition of ≈ 1000 ppm of silicon produced a microstructure that contained only defect-free AlN grains and polytypoid grains.

IV. DISCUSSION

A. AIN-Al₂O₃ polytypoids

Microstructural characterization of the AlN-Al₂O₃ system using CTEM and HRTEM demonstrate the gradual transition from isolated planar and curved IDB's to the ordered polytypoid phases with increasing oxygen content. These polytypoid phases have been studied in detail and have been shown to be periodically alternating IDB's of two distinct types, planar and corrugated. The previously accepted polytypoid model consisting of

arrays of stacking faults is therefore demonstrated to be incorrect. The variation in the microstructure, from extended defect-free grains, to grains containing isolated extended defects, to grains showing mixed populations of extended defects and polytypoid structures, and finally to polytypoid grains, provides evidence showing the inhomogeneous distribution of oxygen within the sample, because the type and density of defects are related to the oxygen concentration within the grain.

A model for the nucleation and growth of these polytypoid phases is proposed, based on the previous studies concerning the formation of the isolated planar and curved IDB's. When the oxygen content in the AlN matrix is sufficiently high, the octahedral complexes precipitate on the basal plane, as described previously in paper II.^{25,30} In the case of polytypoids, the oxygen content in solid solution is very high, and the octahedral complexes precipitate on closely spaced basal planes. As outlined in paper II³⁰ the curved IDB nucleates and grows out from the basal fault, producing the planar and curved IDB's. This process also occurs in the polytypoid phases; however, it is apparent from Fig. 5 that the close proximity of adjacent planar IDB's constrains the growth of the curved IDB, forcing it to lie approximately midway between two planar IDB's, thus forming the corrugated IDB. Also, as shown moving left to right across Fig. 5, as the curved IDB's become more constrained, they consequently become more planar as the distance between planar IDB's decreases.

The TEM micrographs in Fig. 6, 9, and 10 clearly show that the structure of the corrugated IDB interface is nonperiodic. There is no evidence for any periodic structure in either the $\langle 10\overline{1}0 \rangle$ or $\langle 0001 \rangle$ directions. The interface oscillates in the $\langle 0001 \rangle$ between adjacent planar IDB's and exhibits diffuse contrast in the HRTEM images; at lower magnifications, the interface appears to have a finite width of $\approx 2-5$ nm, based upon the contrast at the interface. This variable contrast suggests that there is also no periodicity in the structure on moving through the sample parallel to the incident electron beam. Therefore, the structure is believed to be completely random in all three orthogonal directions. This corrugated interface can be described as a random "dimpled" plane with the dimples being of varying size. This corrugated interface is believed to form in order to minimize the strain associated with the local coordination changes, electrostatic repulsion, and distortion of the lattice caused by the aluminum vacancies necessary for electrical neutrality. Previous work^{29,30,37} indicates that vacancies are repelled from the planar IDB and prefer to cluster at the curved IDB.

An exact model cannot readily be proposed for the structure of the corrugated IDB because of its nonplanar and unpredictable path through the lattice. However, a corrugated IDB structure, based upon arrangements of

partially occupied oppositely pointing tetrahedral sites (The corrugated IDB cannot contain octahedral units such as those in the planar IDB because their presence would result in the introduction of a local change in stacking sequence that would produce a basal plane translation, which was not observed. Also, based upon our arguments in paper II³⁰ for the nucleation of the curved IDB, the presence of octahedral units would cause a second curved IDB to nucleate between the curved and adjacent planar IDB.) can be used to construct an IDB with similar characteristics, an example of which is presented in Fig. 14. Aluminum vacancies have been deliberately omitted from Fig. 14, to aid in clarity. A contraction of the AlN lattice, by as much as 17%, occurs around aluminum vacancies, 23,32 producing lattice strains and distortion. Because of the difficulty in precisely determining the effect of vacancies on distortions of the host wurtize AlN lattice, this effect has not been included in the regular structure portrayed in Fig. 14.

Finally, from this and previous work^{23,27,29,30,37} a complete understanding has been developed that can explain the mechanism by which oxygen gradually transforms hexagonal AlN (tetrahedral coord.) to the cubic spinel γ -AlON structure (mixed tetrahedral, octahedral coord.) As the oxygen concentration increases, the spacing between planar and corrugated IDB's decreases, such that less and less crystal with the hexagonal AlN structure lies between the IDB's. It is important to note that the structural features present in the two IDB in-

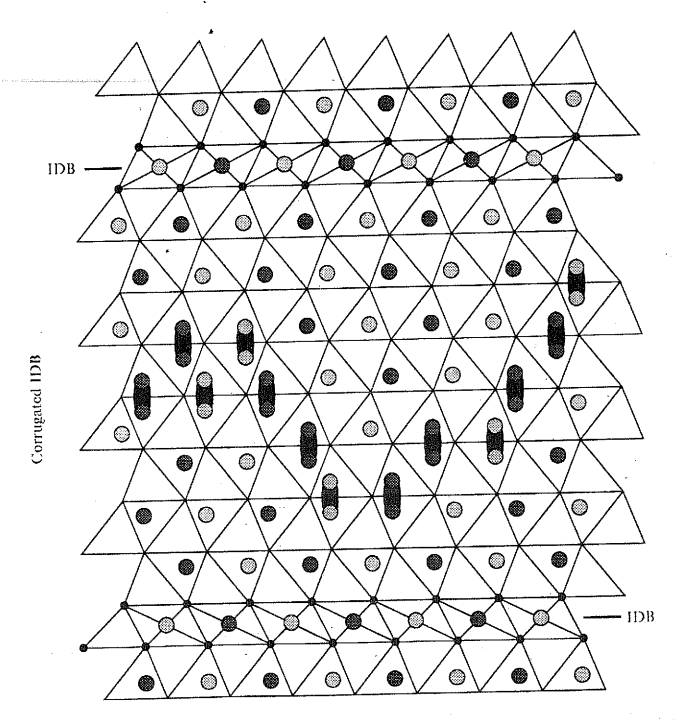


FIG. 14. Model of the $AlN-Al_2O_3$ polytypoid comprised of planar IDB's and a schematic of a representative corrugated IDB (distortions due to different bond lengths and the presence of aluminum vacancies have been omitted for clarity).

terfaces comprising the polytypoid structure, octahedral coordination at the planar IDB, and oppositely pointing filled tetrahedral sites at the corrugated IDB, are both present in the cubic spinel γ -AlON structure. In fact, the γ -AlON structure when viewed along an $\langle hk0 \rangle$ reveals the structure to be comprised of alternating octahedral and tetrahedral coordinated layers. Therefore, it is surmised that at sufficiently high oxygen concentrations the spacing between the planar and corrugated IDB's becomes zero, at which point they contact each other, forming the cubic spinel structure. At these very high oxygen concentrations the constraint imposed upon the corrugated IDB by its adjacent planar IDB's forces it to be planar. An interesting question that currently is unanswered is does a similar gradual structural transformation occur on moving from mixed octahedral and tetrahedral bonding in γ -AlON to all octahedral bonding in Al₂O₃, and if so, is the process similar to that outlined above, involving arrays of impurity-controlled extended defects.

B. AIN-Al₂O₃-SiO₂ "SiAION" polytypoids

The effect of silicon on the structure of the polytypoids is shown by comparison of Fig. 9 and 12. Figure 9 shows the polytypoid structure in the AlN-Al₂O₃ system to be composed of alternating planar and corrugated IDB's. Figure 12 shows the strikingly different polytypoid structure that exists in samples that contain silicon. The silicon-containing polytypoid has two types of planar IDB: IDB-P and IDB-P'. Also, the corrugated IDB present in the AlN-Al₂O₃ polytypoid is not apparent in the silicon-containing samples. However, close inspection of the silicon polytypoid in Fig. 13 revealed atomic planes of high intensity that were always present between the different planar IDB's. These regions are suspected to be the corrugated IDB's that have become more planar in structure. Therefore, it would appear that the curved IDB becomes corrugated when constrained, and more planar with the addition of silicon. The nature of the two high intensity planes adjacent to the IDP-P has not yet been determined.

It is apparent from these observations that silicon has a strong influence on controlling the polytypoid structure by forming the second planar IDB-P' and significantly adjusting the structure of the corrugated IDB. Additional supporting evidence for the influence of silicon was obtained from the fact that ordered polytypoid grains were much more common in silicon-containing samples than in AlN-Al₂O₃ samples, and from nuclear magnetic resonance (NMR) studies in the literature.³⁸ These observations indicate that silicon modifies the polytypoid structure, creating an energetically more stable structure compared to polytypoid structures that do not contain silicon. The precise manner in which silicon modifies the polytypoid structure is unclear. However, silicon could

adjust the charge neutrality of the crystal by removing aluminum vacancies. Because the corrugated IDB structure contains aluminum vacancies, any reduction in the aluminum vacancy concentration would affect the structure of the corrugated IDB, as is observed in the silicon-containing polytypoids.

ral

ng

)th

he

als

ral

ır-

ns

3's

er

gh

he

to

ın-

on

ral

 $)_3$

ve.

:ts.

lv-

12.

ıar

зlу

hat

ıas

the

lis

er.

13

iys

re-

ive

uld

ien

on.

to

188

ure

itly

nal

vas

ins

les

etic

b-

oid

ure

ain

the

uld

Studies of SiAlON polytypoids and β' -Sialon, using ²⁷Al and ²⁹Si high-speed magic angle spinning (MAS) NMR,³⁸ indicate that a strict bonding preference exists for Si–N and Al–O in β' -Sialon, demonstrating that this structure is formed from microdomains of Si–N and Al–O bonded regions. The data from 15 R and 21R SiAlON polytypoids were found to be more difficult to interpret, but revealed that these structures were comprised of mainly AlN₄ structural units. Strong preference was found for oxygen to bond preferentially with aluminum, forming AlO₆ octahedral and AlN₃O tetrahedral units, rather than for oxygen to bond with silicon. The preferred structural unit for silicon was SiN₄, with a very small amount of SiN₃O also present.

Based upon the observed strong effect of silicon on the polytypoid structure, the direct observation of the structure by HRTEM, and the NMR data from the literature, structural models for SiAlON polytypoids are being developed. The primary candidates for the IDB-P' interface structure are layers of either β -Si₃N₄³⁹ or Si_2N_2O ,⁴⁰ which are the parent structures of β' -Sialon and O-Sialon, respectively.⁴ The first model for the IDB-P' is based upon the insertion of a half layer of β -Si₃N₄ into the wurtzite AlN lattice. The c-axis of the AlN host lattice lies parallel to the c-axis of the β -Si₃N₄, and the basal planes of the AlN and $\beta - Si_3N_4$ also lie parallel such that the $\langle 1\overline{1}00 \rangle$ and $\langle 1\overline{2}10 \rangle$ directions of both crystals are coincident. A small lattice mismatch, <1.5%, can be achieved with two β -Si₃N₄ unit cells matching five AlN unit cells. An alternative model supposes that a half layer of Si₂N₂O is inserted into the AlN lattice. The a-axis of the Si₂N₂O structure lies parallel to the c-axis of the wurtzite structure, and the (100) plane of the Si₂N₂O lattice is parallel with the basal plane of the wurtzite structure. The $\langle 010 \rangle$ and (021) directions in the Si₂N₂O structure are coincident with the $\langle 1100 \rangle$ and $\langle 1210 \rangle$ directions of the AlN lattice. Small adjustments in the lattice parameter of Si₂N₂O <5% are required to match the lattice parameter of the wurtzite basal plane. The above models and the calculated lattice mismatches are based upon an ideal pure AlN lattice containing no impurities. However, the presence of dissolved oxygen is known to decrease the a-axis lattice parameter of the wurtzite lattice making the above calculated lattice mismatches smaller, 4,23 and possibly removing them completely. It is expected that the IDB-P' interface will be strained slightly. Both models provide an inversion across the interface, and assume that silicon bonds preferentially with nitrogen, in

agreement with the NMR results. A model is also being developed to describe the structure of the corrugated IDB present in the silicon-containing polytypoids.

A recent study by Redlich, 41 using PEELS, clearly shows oxygen segregation to both planar and corrugated IDB's, as has been previously reported. 22,26,28,30 In this same study, oxygen profiles obtained from a 27R AlN-Al₂O₃ polytypoid structure indicated oxygen segregation only at the planar interfaces in the structure: no mention was made of corrugated IDB's lying between the planar IDB's. However, no detailed multibeam diffraction experiments were performed to investigate for the possible presence of the corrugated IDB, or to show that the planar interfaces were IDB's, as reported in this paper. Two possibilities exist, based upon the study of Redlich. First, oxygen does not segregate to the corrugated IDB once constrained within the polytypoid structure; this would explain why no oxygen segregation was observed between the planar IDB's. Second, the corrugated IDB was not present in their samples. These discrepancies require further investigation by AEM, which would also allow measurement of silicon segregation at the planar IDB-P' and silicon distribution within the silicon-containing polytypoids.

The experimental CTEM and HRTEM studies, as well as the initial atomistic simulations reported here, provide incontrovertible evidence that the previously accepted model of Jack⁴ is incorrect, and offers independent confirmation of the basic structure proposed by Thompson, with some necessary changes. Also, they indicated that the preferred polytypoid structures are comprised of periodic arrays of IDB's. Additional calculations would be of great value in further analyzing the $AlN-Al_2O_3$ and silicon-containing polytypoid structures. This work presented here demonstrates a progressive sequence showing the gradual transformation of the hexagonal AlN wurtzite structure to the γ -AlON cubic spinel structure, via oxygen incorporation at extended two-dimensional defects.

The overwhelming evidence presented here indicate that polytypoid phases in the AlN-Al₂O₃ system and the Si₃N₄-SiO₂-AlN-Al₂O₃ system are periodic arrays of IDB's. Also, a recent report showed the existence of isolated IDB's in α' -SiAlON.⁴² Therefore, based upon these observations, the nature of the polytypoid structures of other metal-SiAlON systems is brought into question and require reexamination. The current definition of a polytypoid does not clearly define the crystallographic nature of the interface. The work presented here clearly shows that a change in stacking sequence does occur across the interfaces; however, the present interfaces are inversion rather than purely translational in nature, as would be the case for a true stacking fault. Both types of interfaces can cause a change in the stacking sequence between adjacent blocks of crystal. It

is the liberal use of the definition of the stacking fault as a region of crystal across which the stacking changes that has led to the current misunderstanding. We propose that the definition of a polytypoid be altered to describe the interface as an interface across which the stacking sequence changes by any type of crystallographic operation, e.g., translation, inversion, rotation, or mirror. An alternative is to classify those interfaces comprised of compositionally induced translational interfaces as polytypoids, such that this remains a subset of polytypes, and to classify those structures comprised of arrays of inversion domain boundaries, be they all the same or different in structure, as polar-polytypoids.

V. CONCLUSIONS

(1) The structure of the polytypoid phases that exist in the AlN-Al₂O₃ system and in the AlN-rich corner of the SiAlON phase diagram has been shown to be inversion domain boundaries, not stacking faults.

(2) The structure of the polytypoid in the AlN–Al₂O₃ system are comprised of alternating planar IDB's and corrugated IDB's. The planar IDB is identical to that found in AlN containing a low oxygen concentration. A model for the structure of the corrugated IDB is presented, and is based upon the sharing of partial-filled tetrahedral sites pointing in opposite directions and segregation of aluminum vacancies.

(3) The structure of polytypoids containing silicon in the $AlN-Al_2O_2-SiO_2$ system is also comprised of two different types of IDB, IDB-P, and IDB-P', which were separated by a corrugated IDB whose structure has become planar. The IDB-P is identical to the planar IDB in the $AlN-Al_2O_3$ system. Preliminary models for the IDB-P' based upon $\beta-Si_3N_4$ and Si_2N_2O are proposed. Silicon is observed to have a strong effect on altering the structure of the corrugated IDB with very small amounts of silicon changing the structure of the corrugated IDB to a more planar structure.

(4) The previously accepted model of Jack which describes SiAlON polytypoids as periodic arrays of stacking faults is therefore shown to be incorrect. The results presented here regarding the structure of the polytypoids support with some minor changes the model proposed by Thompson for SiAlON polytypoids.

(5) In a more general context, the liberal definition of interfaces across which the stacking sequence changes as stacking faults without specifying their inversion or translation should be disallowed, and it would be beneficial to refine the definition of polytypoid structures, either by making the definition cover a broader class of interfaces, or by introducing a new category of polytypoids whose interfaces are only arrays of inversion domain boundaries—polar-polytypoids.

ACKNOWLEDGMENTS

The authors wish to thank the Semiconductor Research Corporation (SRC) and British Petroleum America for funding this work, and the external users program at the Center for High-Resolution Electron Microscopy at Arizona State University.

REFERENCES

- K. H. Jack and W. I. Wilson, Nature Phys. Sci. (London) 238, 28 (1972)
- 2. Y. Oyama and O. Kamigaito, Jpn. J. Appl. Phys. 10, 1637 (1971).
- S. W. Bailey, V. A. Frank-Kamenetskii, S. Goldsztaub, A. Kato, H. Schulz, A. Pabst, H. Schulz, H. F. W. Taylor, M. Fleischer, and A. J. C. Wilson, Acta Crystallogr. A 33, 681–684 (1977).
- 4. K. H. Jack, J. Mater. Sci. 11, 1135-1158 (1976).
- L. J. Gauckler, H. L. Lukas, and G. Petzow, J. Am. Ceram. Soc. 58, 346–347 (1975).
- 6. K. Komeya and A. Tsuge, Yogyo-Kyokai-Shi **89**, 615-620 (1981)
- D. P. Thompson, P. Korgul, and S. Hendry, in *Progress in Nitrogen Ceramics, NATO Advanced Studies Institute, Series E: Applied Science No. 65*, edited by F. L. Riley (Martinus Nijhoff Publishers, The Hague, The Netherlands, 1983), pp. 61–74.
- B. Bergman, T. Ekstrom, and A. Micski, J. Eur. Ceram. Soc. 8, 141–151 (1991).
- H. K. Zhaung, W. L. Li, J. W. Feng, Z. K. Huang, and D. S. Yan, J. Eur. Ceram. Soc. 7, 329–333 (1991).
- T. Ekstrom and M. Nygren, J. Am. Ceram. Soc. 75, 259-276 (1992).
- 11. D.P. Thompson, J. Mater. Sci. Lett. 11, 1377-1380 (1976).
- D. P. Thompson, in Nitrogen Ceramics, NATO Advanced Studies Institute, Series E: Applied Science No. 23, edited by F. L. Riley (Noordhoff International Publishing, Leyden, The Netherlands, 1977), pp. 129–135.
- D. R. Clark, T. M. Shaw, and D. P. Thompson, J. Mater. Sci. Lett. 13, 217–219 (1978).
- 14. D. P. Thompson, Mater. Sci. Forum 47, 21-42 (1989).
- G. Van Tendeloo, K. T. Faber, and G. Thomas, J. Mater. Sci. 18, 525-532 (1983).
- Y. Bando, M. Mitomo, Y. Kitami, and F. Izumi, J. Microsc. 142, 235–246 (1986).
- 17. K. M. Krishnan, R. S. Rai, G. Thomas, N. D. Corbin, and J. W. McCauley, in *Defect Properties and Processing of High-Technology Nonmetallic Materials*, edited by Y. Chen, W. D. Kingery, and R. J. Stokes (Mater. Res. Soc. Symp. Proc. 60, Pittsburgh, PA, 1986), pp. 211-218.
- 18. S. F. Bartram and G. A. Slack, Acta Crystallogr. B **35**, 2281–2283 (1979).
- P. Sainz de Baranda, A. K. Knudsen, and E. Ruh, J. Am. Ceram. Soc. 76, 1761–1771 (1993).
- S. McKernan and C. B. Carter, in Advanced Electronic Packaging Materials, edited by A. T. Barfknecht, J. P. Partridge, C. J. Chen. and C-Y. Li (Mater. Res. Soc. Symp. Proc. 167, Pittsburgh, PA, 1990), pp. 289–294.
- A. D. Westwood and M. R. Notis, in *Advanced Electronic Packaging Materials*, edited by A. T. Barfknecht, J. P. Partridge, C. J. Chen, and C-Y. Li (Mater. Res. Soc. Symp. Proc. 167, Pittsburgh, PA, 1990), pp. 295–300.
- R. A. Youngman, J. H. Harris, P. A. Labun, R. J. Graham, and J. K. Weiss, in *Advanced Electronic Packaging Materials*, edited by A. T. Barfknecht, J. P. Partridge, C. J. Chen, and C-Y. Li (Mater. Res. Soc. Symp. Proc. 167, Pittsburgh, PA, 1990), pp. 301–306.

- 23. J.H. Harris, R. A. Youngman, and R. G. Teller, J. Mater. Res. 5, 1763–1773 (1990).
- 24. A. Berger, J. Am. Ceram. Soc. 74, 1148-1151 (1991).

m

28

.to.

ınd

oc.

520

E: off

an, 276

lies ley ids,

18, 42, and *gh*-.D. 60,

am.

ing ien, PA,

uck-J. J. igh,

ter.

- A. D. Westwood and M. R. Notis, J. Am. Ceram. Soc. 74, 1226–1239 (1991).
- A. D. Westwood, J. R. Michael, and M. R. Notis, in *Microbeam Analysis 1991*, edited by D. G. Howitt (San Francisco Press, San Francisco, CA, 1991), pp. 245–249.
- M. R. McCartney, R. A. Youngman, and R. G. Teller, Ultramicroscopy 40, 291–299 (1992).
- A. D. Westwood, J. R. Michael, and M. R. Notis, J. Microsc. 167, 287–302 (1992).
- 29. A.D. Westwood, R.A. Youngman, M.R. McCartney, A.N. Cormack, and M.R. Notis, J. Mater. Res. 10, 1270 (1995).
- A. D. Westwood, R. A. Youngman, M. R. McCartney, A. N. Cormack, and M. R. Notis, J. Mater. Res. 10, 1287 (1995).
- R. A. Youngman, A. D. Westwood, and M. R. McCartney, in Defect-Interface Interactions, edited by E. P. Kvam, A. H. King, M. J. Mills, T. D. Sands, and V. Vitek (Mater. Res. Soc. Symp. Proc 319, Pittsburgh, PA, 1994), pp. 45-50.
- 32. G. A. Slack, J. Phys. Chem. Solids 34, 321-335 (1973).

- S. Amelinckx and J. Van Landhuyt, in *Diffraction and Imaging Techniques in Materials Science*, edited by S. Amelinckx,
 R. Gevers, and J. Van Landuyt (North-Holland Publishing Company, Amsterdam, The Netherlands, 1978), pp. 107–151.
- 34. R. Serneels, M. Snykers, P. Delavignette, R. Gevers, and S. Amelinckx, Phys. Status Solidi B 58, 277–292 (1973).
- M. Snykers, R. Serneels, P. Delavignette, R. Gevers, J Van Landuyt, and S. Amelinckx, Phys. Status Solidi A 41, 51-63 (1977).
- W. Coene, G. Janssen, M. Op de Beeck, and D. Van Dyke, Phys. Rev. Lett. 69, 3743-3746 (1992).
- 37. A. D. Westwood, Ph.D. Thesis, Lehigh University, Bethlehem, PA (1992), available through UMI dissertation services.
- 38. M. E. Smith, J. Phys. Chem. 96, 1444-1448 (1992).
- 39. R. Grun, Acta Crystallogr. B 35, 800-804 (1979).
- I. Idresedt and C. Brosset, Acta Chem. Scand 18, 1879–1886 (1964).
- 41. P. Redlich, Masters Thesis, Max-Planck Institut fur Metall-forschung, Stuttgart, Germany (1993).
- 42. S. Hwang and I-W. Chen, J. Am. Ceram. Soc. **77**, 1719-1728 (1994).